^{18}F-Fluorodeoxyglucose-Positron Emission Tomography/Computed Tomography in Tuberculosis: Spectrum of Manifestations

Abstract

The objective of this article is to provide an illustrative tutorial highlighting the utility of ^{18}F-fluorodeoxyglucose-positron emission tomography/computed tomography (^{18}F-FDG-PET/CT) imaging to detect spectrum of manifestations in patients with tuberculosis (TB). FDG-PET/CT is a powerful tool for early diagnosis, measuring the extent of disease (staging), and consequently for evaluation of response to therapy in patients with TB.

Keywords: *Fluorodeoxyglucose-positron emission tomography/computed tomography, positron emission tomography/computed tomography, tuberculosis*

Krishan Kant Agarwal, Abhishek Behera, Rakesh Kumar[1], Chandrasekhar Bal

Department of Nuclear Medicine, All India Institute of Medical Sciences, [1]Department of Nuclear Medicine, Division of Diagnostic Nuclear Medicine, All India Institute of Medical Sciences, New Delhi, India

Introduction

Tuberculosis (TB) is contagious and airborne infectious disease. It ranks as the second leading cause of death from a single infectious agent, after the human immunodeficiency virus. Over past two decades, TB remains a worldwide emergency despite substantial improvement in health service. Patients with sputum-negative pulmonary TB (PTB) and extra-PTB (EPTB) are difficult to diagnose and may be missed at all points of care. Imaging for diagnosis of TB is challenging because it can mimic other diseases such as sarcoidosis or neoplasm.

Various radiopharmaceuticals used in positron emission tomography (PET) imaging have shown potential utility in TB. The most commonly used PET radiotracer in the management of TB is ^{18}F-fluorodeoxyglucose (^{18}F-FDG). FDG is a surrogate marker for glucose metabolism and has consistently been shown to have increased concentration in areas of inflammation associated with active TB. ^{18}F-FDG-PET/computed tomography (CT) though unable to differentiate between TB and other diseases may still have a role in TB diagnosis in conjunction with other modalities. Increasingly, PET/CT is being used to accurately define the full extent of systemic involvement, yield material for culture and sensitivity studies (to allow an early diagnosis of drug-resistant TB), or potentially to monitor the healing process. PET/CT scans may suggest the sites of safe high-yield biopsies, thus yielding confirmatory histopathology, cultures, or polymerase chain reaction samples.[1,2]

Fluorodeoxyglucose-positron Emission Tomography/Computed Tomography Findings in Tuberculosis

Pulmonary tuberculosis

Parenchymal involvement:

- ^{18}F-FDG-PET/CT showed tracer uptake in areas of lung consolidation ± cavitations surrounded by micronodules and mild uptake within lymph nodes. ^{18}F-FDG-PET is able to differentiate active PTB from old or inactive disease as active tuberculoma has significantly higher maximum standardized uptake value compared with inactive tuberculoma.[3] ^{18}F-FDG-PET/CT has the potential to become a tool for monitoring the treatment response in selected cases of EPTB or multidrug resistance. PET/CT scans can guide accurate targeting of active sites of disease for biopsy, from the thoracic cavity as well [Figures 1-4]
- Lymphadenopathy: FDG avidity with necrosis and calcification may be seen in involved lymph nodes with or without parenchymal lung involvement [Figure 5]. On CT, the enlarged nodes typically show central low attenuation, which represents caseous necrosis, and peripheral rim enhancement, which represents the vascular rim of the granulomatous inflammatory tissue

How to cite this article: Agarwal KK, Behera A, Kumar R, Bal C. 18F-fluorodeoxyglucose-positron emission tomography/computed tomography in tuberculosis: Spectrum of manifestations. Indian J Nucl Med 2017;32:316-21.

Address for correspondence:
Dr. Rakesh Kumar, Department of Nuclear Medicine, Division of Diagnostic Nuclear Medicine, All India Institute of Medical Sciences, New Delhi - 110 029, India.
E-mail: rkphulia@yahoo.com

Access this article online

Website: www.ijnm.in

DOI: 10.4103/ijnm.IJNM_29_17

Quick Response Code:

- Pleural effusion: Pleural effusion may be associated with parenchymal lung involvement or may be present independently. Pleural effusion is usually unilateral and on the same side as the primary focus of TB. The effusion may be large and occur in patients without evidence of parenchymal disease on chest radiographs. The effusion may show mild FDG uptake.

Cardiac tuberculosis

Cardiac TB usually presents as pericardial involvement in the form of pericardial thickening [Figure 3]. Effusions are reportedly less common. Myocardial involvement may be difficult to discern due to physiological FDG uptake and may potentially benefit from dietary preparation aimed at reducing physiological myocardial FDG uptake.[4]

Musculoskeletal tuberculosis

- Bone involvement: Skeletal TB usually occurs secondary to hematogenous spread from other lesions. Spinal TB forms the most common form of skeletal TB forming approximately 50% cases of skeletal

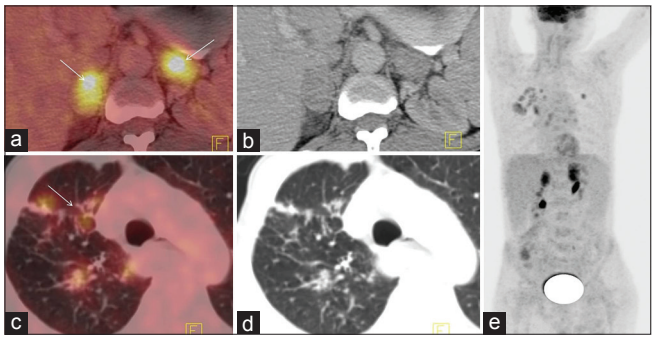

Figure 1: A 55-year-old male presented with anorexia and weight loss. (a and b) Axial fluorodeoxyglucose-positron emission tomography/computed tomography and computed tomography images show soft tissue density lesions in both adrenal glands with necrotic areas and increased tracer uptake (arrows). (c and d) Axial fluorodeoxyglucose-positron emission tomography/computed tomography and computed tomography images show fibro-cavitatory changes and fibro-parenchymal opacities in the right lung upper lobe with increased tracer uptake (arrow). (e) Maximum intensity projection 18F-fluorodeoxyglucose-positron emission tomography image shows metabolically active disease involving right lung and both adrenal glands suggestive of tubercular etiology

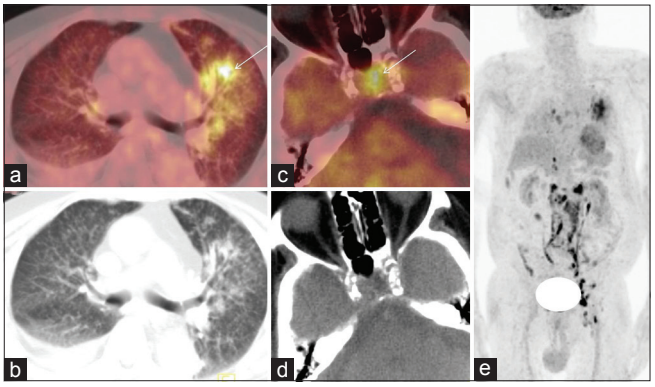

Figure 2: A 74-year-old male presented with anorexia and weight loss, suspicious for disseminated tuberculosis. (a and b) Axial fluorodeoxyglucose-positron emission tomography/computed tomography and computed tomography images show centrilobular nodular lesions in both lungs with increased tracer uptake and peribronchovascular thickening and ground glassing in the left lung upper lobe showing fluorodeoxyglucose uptake (arrows). (c and d) Axial fluorodeoxyglucose-positron emission tomography/computed tomography and computed tomography images show soft tissue thickening with increased fluorodeoxyglucose uptake in the sellar region (arrow). (e) Maximum intensity projection 18F-fluorodeoxyglucose-positron emission tomography image shows metabolically active disease involving both lungs with retroperitoneal, pelvic, and left inguinal lymphadenopathy suggestive of tubercular etiology

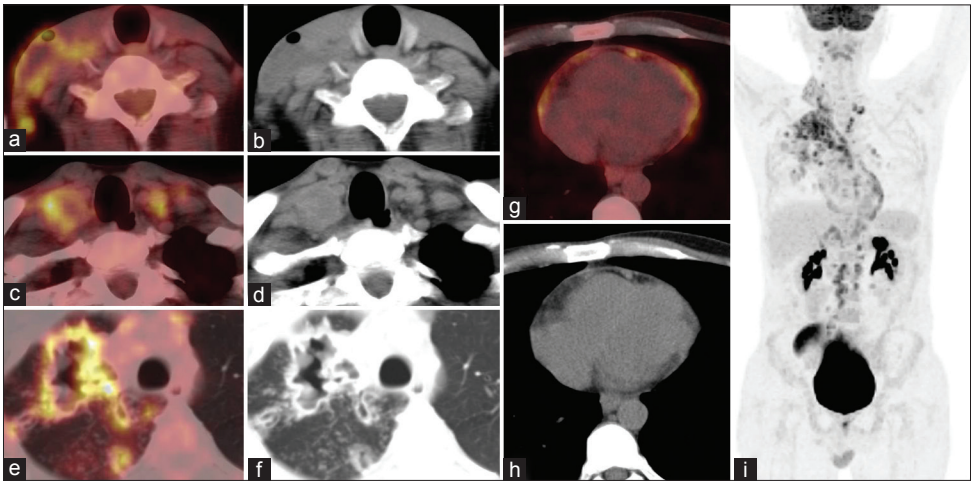

Figure 3: A 35-year-old male presented with multifocal tuberculosis. (a and b) Axial fluorodeoxyglucose-positron emission tomography/computed tomography and computed tomography images show cold abscess along the posterior border of the right sternocleidomastoid muscle showing peripheral fluorodeoxyglucose uptake with an air pocket. (c and d) Axial fluorodeoxyglucose-positron emission tomography/computed tomography and computed tomography images show bilateral supraclavicular lymph nodes (right > left) with necrotic areas and increased tracer uptake. (e and f) Axial fluorodeoxyglucose-positron emission tomography/computed tomography and computed tomography images show confluent irregular cavitatory lesion in the right lung upper lobe with few adjacent cavitatory lesions showing increased tracer uptake. (g and h) Axial fluorodeoxyglucose-positron emission tomography/computed tomography and computed tomography images show irregular nodular thickening of the pericardium showing increased tracer uptake (arrow). (i) Maximum intensity projection 18F-fluorodeoxyglucose-positron emission tomography image shows metabolically active pathology involving right cervical, bilateral supraclavicular, mediastinal, retroperitoneal lymphadenopathy, both lungs (right > left), pericardium, and cold abscess along right sternocleidomastoid muscle suggestive of multifocal active tubercular pathology

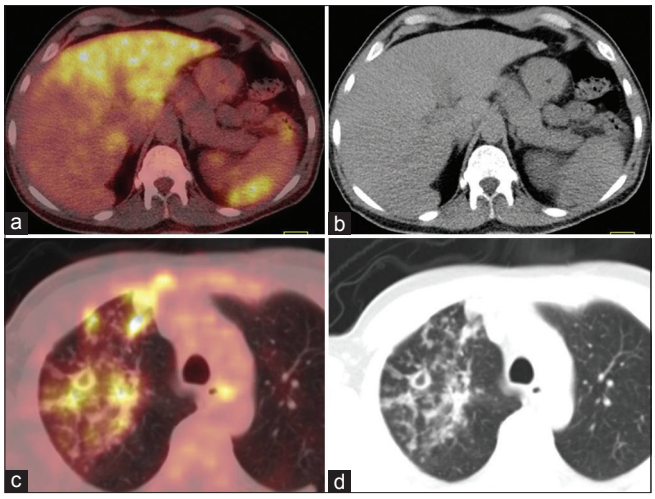

Figure 4: A 35-year-old male presented with sputum positive tuberculosis. He was on antitubercular therapy for 15 days. He was referred for 18F-fluorodeoxyglucose-positron emission tomography/computed tomography scan to know extent of disease. (a and b) Axial fluorodeoxyglucose-positron emission tomography/computed tomography and computed tomography images show hypodense lesions involving left lobe of the liver and increased tracer uptake. (c and d) Axial fluorodeoxyglucose-positron emission tomography/computed tomography and computed tomography images show fibro-cavitatory changes and fibro-parenchymal opacities in the right lung upper lobe with increased tracer uptake suggestive of active tubercular pathology

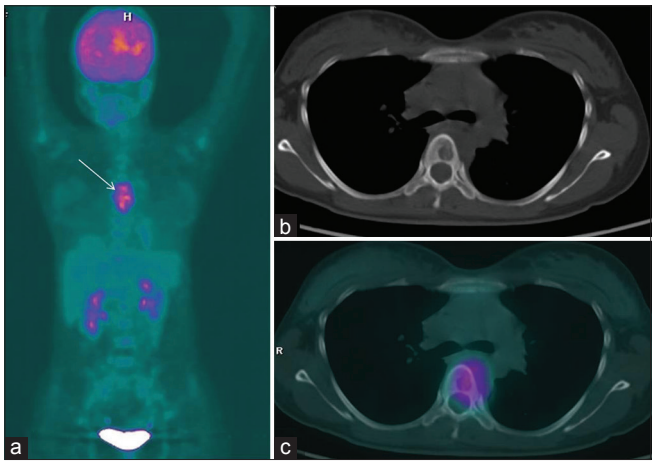

Figure 6: A 23-year-old female presented with fever and back pain. (a) Maximum intensity projection 18F-fluorodeoxyglucose-positron emission tomography image shows metabolically active lesion in dorsal vertebra region suggestive of active. Pott's spine pathology (arrows). (b and c) Axial fluorodeoxyglucose-positron emission tomography/computed tomography and computed tomography images show lytic lesion with paravertebral soft tissue component involving body of dorsal vertebra with increased tracer uptake

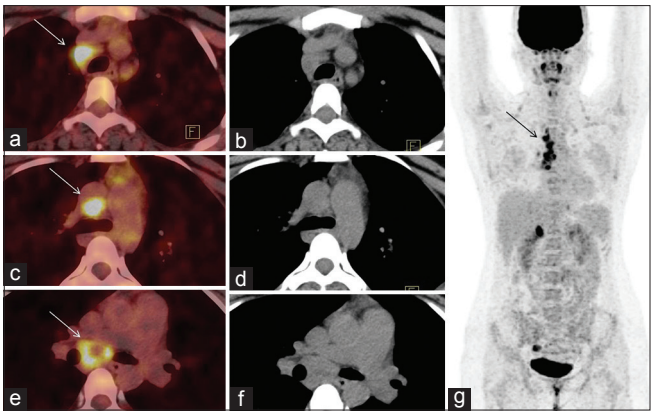

Figure 5: A 20-year-old female presented with sputum-negative tuberculosis. He was on antitubercular therapy. He was referred for 18F-fluorodeoxyglucose-positron emission tomography/computed tomography scan to know active status of tubercular pathology. (a and b) Axial fluorodeoxyglucose-positron emission tomography/computed tomography and computed tomography images show enlarged right paratracheal lymph node with necrosis and increased tracer uptake (arrows). (c and d) Axial fluorodeoxyglucose-positron emission tomography/computed tomography and computed tomography images show pretracheal lymph node with necrosis and increased tracer uptake (arrow). (e and f) Axial fluorodeoxyglucose-positron emission tomography/computed tomography and computed tomography images show enlarged subcarinal lymph node with central necrosis and peripheral tracer uptake (arrow). (g) Maximum intensity projection 18F-fluorodeoxyglucose-positron emission tomography image shows metabolically active mediastinal (arrow) and periportal lymphadenopathy suggestive of active residual tubercular pathology

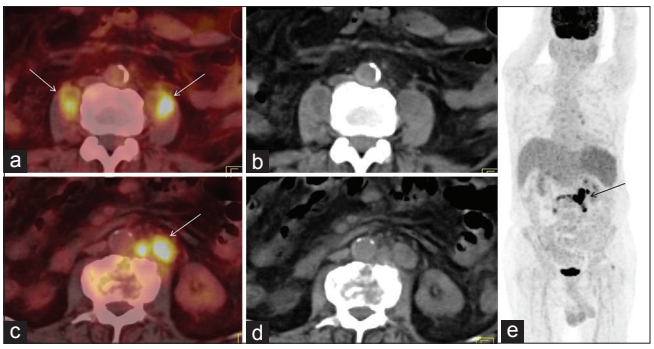

Figure 7: A 75-year-old male presented with anorexia and weight loss. (a and b) Axial fluorodeoxyglucose-positron emission tomography/computed tomography and computed tomography images show intramuscular fluid collection in both psoas muscles with increased radiotracer uptake suggestive of metabolically active cold abscess (arrows). (c and d) Axial fluorodeoxyglucose-positron emission tomography/computed tomography and computed tomography images show few enlarged paraaortic lymph nodes at L2/L3 level with increased tracer uptake (arrow). (e) Maximum intensity projection 18F-fluorodeoxyglucose-positron emission tomography image shows metabolically active paraaortic lymph nodes with cold abscess in both psoas muscles suggestive of tubercular etiology (arrow)

TB [Figure 6]. Paradiscal FDG avid lesions with associated cold abscess are the most frequent. Vertebral compression, collapse, and associated deformity may occur. Hip and knee joints form other commonly involved sites of skeletal TB. Involvement of the ankle, shoulder, and elbow may also occur, though far rarer. Involvement of the small bones of the hands and feet may lead to dactylitis. Tubercular osteomyelitis in the absence of arthritis is rare. It has been described as a poorly defined lytic lesion with peripheral sclerosis on imaging[5]

- Muscle involvement: Muscle involvement may occur either as contiguous involvement from adjacent focus of TB or as an independent focus of infection in the muscle. Involvement is usually in the form of an FDG avid cold abscess. The lesions tend to spread along the

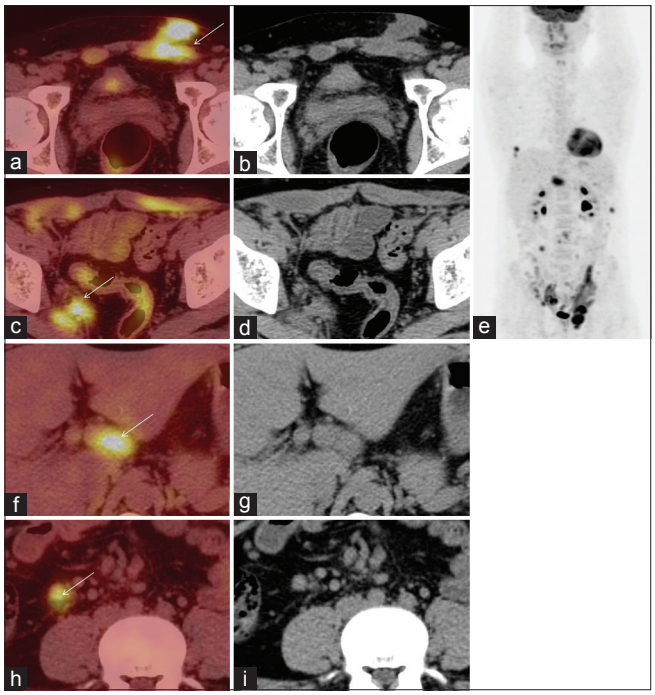

Figure 8: A 20-year-old male presented with abdominal tuberculosis. He was on antitubercular therapy. He was referred for 18F-fluorodeoxyglucose-positron emission tomography/computed tomography scan to know active status of tubercular pathology. (a and b) Axial fluorodeoxyglucose-positron emission tomography/computed tomography and computed tomography images show intramuscular fluid collection in both rectus muscles with increased radiotracer uptake and sinus formation in the left pubic region suggestive of metabolically active cold abscess with sinus formation (arrows). (c and d) Axial fluorodeoxyglucose-positron emission tomography/computed tomography and computed tomography images show few enlarged right internal iliac and external iliac group of lymph nodes with increased tracer uptake (arrow). (e) Maximum intensity projection 18F-fluorodeoxyglucose-positron emission tomography image shows metabolically active abdominal, retroperitoneal, and pelvic lymphadenopathy with cold abscess in both rectus muscles with sinus formation suggestive of active tubercular pathology. A 20-year-old male presented with abdominal tuberculosis. (f and g) Axial fluorodeoxyglucose-positron emission tomography/computed tomography and computed tomography images show periportal lymph nodes with necrotic areas and increased tracer uptake. (h and i) Axial fluorodeoxyglucose-positron emission tomography/computed tomography and computed tomography images show mesenteric lymph nodes with specs of calcification and increased tracer uptake

route offering least resistance and thus track along the fascial planes [Figures 3, 7, and 8].

Tuberculosis involving central nervous system

- Meningeal involvement: Usually seen as involvement of the basal cisterns in the form of basal exudates. Involved areas show contrast enhancement on contrast-enhanced CT. FDG uptake may be seen in involved areas. Choroid plexus enhancement with ventricular enlargement on imaging is highly suggestive of TB meningitis
- Parenchymal involvement: Parenchymal involvement may occur in the form of a tuberculoma, visualized as a ring-enhancing lesion with increased peripheral FDG uptake [Figure 9]. Other forms of involvement include focal cerebritis visualized as a region of increased FDG uptake in brain parenchyma. Cerebritis may progress to form an abscess. Miliary nodules may be seen cases of diffuse miliary TB.[6]

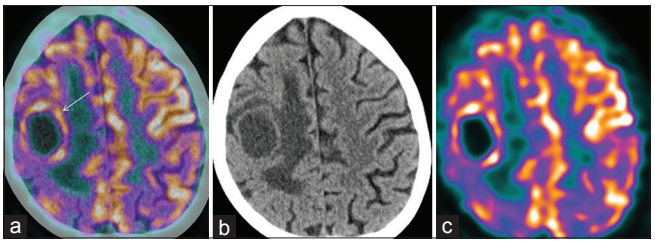

Figure 9: A 15-year-old male presented with fever and seizure. (a-c) Axial fluorodeoxyglucose-positron emission tomography/computed tomography, computed tomography, and positron emission tomography images show hypodense lesion with peripheral tracer uptake in the right frontoparietal region with perilesional edema suggestive of active tubercular pathology

Head and neck tuberculosis

Head and neck TB occurs in about 15% of EPTB:

- Lymph node involvement: Most common location of head and neck TB is within neck nodes. They present as painless cervical lymphadenitis. The involved nodes are homogeneous with central necrosis and calcification. In FDG-PET/CT, they show peripheral increased tracer uptake [Figures 3 and 10]
- Extranodal tuberculosis: Extranodal TB is very rare. The most common affected sites are larynx, temporal bone, and pharynx.

Abdominal tuberculosis

- Lymphadenopathy: Lymphadenopathy is the most common presentation of abdominal TB. In TB, the mesenteric, mesenteric root, celiac, porta hepatis and peripancreatic lymph nodes are most commonly involved, reflecting the lymphatic drainage of the small bowel. Caseating lymph nodes are seen as having hypodense centers and peripheral rim enhancement and increased tracer uptake on FDG-PET/CT [Figures 2, 3 and 8]
- Tuberculous peritonitis: Can be visualized as diffusely FDG avid peritoneal thickening and nodules on fused PET/CT images.[7] Omental thickening is seen often as an omental cake appearance. A fibrous wall can cover the omentum, developing from long-standing inflammation and is called omental line
- Bowel tuberculosis: Better visualized with PET/CT enterography and usually seen as areas of focal FDG uptake with associated thickening/ulceration. Most common site is the ileocaecal region followed by gastroduodenal, colonic, and anorectal region. In early disease, there is symmetric circumferential thickening of cecum and terminal ileum. Later, the ileocaecal valve and adjacent medial wall of the cecum are asymmetrically thickened. In more advanced disease, gross wall thickening, adherent loops, large regional nodes, and mesenteric thickening can together form a soft tissue mass centered around the ileocaecal junction. CT scan can also pick up ulceration or nodularity

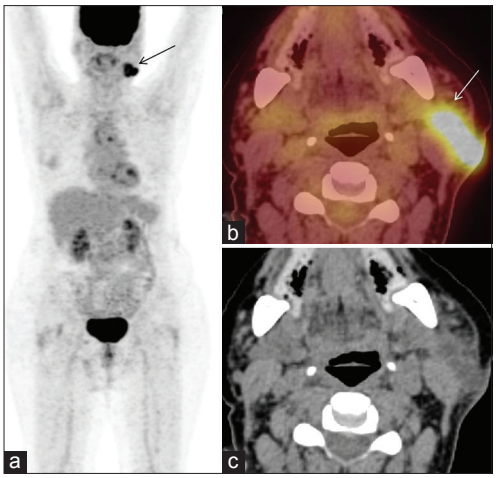

Figure 10: A 78-year-old female presented with left cervical lymphadenopathy. (a) Maximum intensity projection 18F-fluorodeoxyglucose-positron emission tomography image shows metabolically active left cervical lymphadenopathy (arrow). (b and c) Axial fluorodeoxyglucose-positron emission tomography/computed tomography and computed tomography images show heterogeneous necrotic lesion with increased tracer uptake in the left cervical region, extending laterally to subcutaneous and cutaneous plane and skin likely tubercular pathology with abscess formation (arrow)

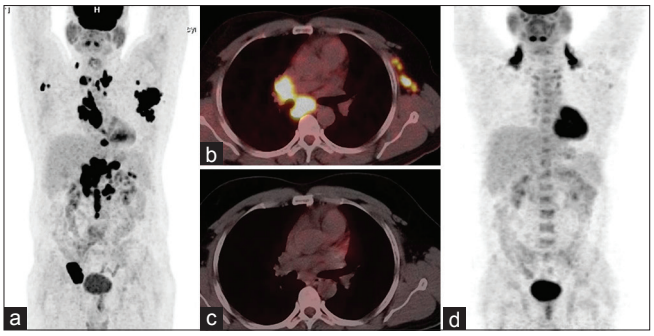

Figure 12: A 32-year-old male presented with disseminated tuberculosis. He was on antitubercular therapy for 6 months. He was referred for 18F-fluorodeoxyglucose-positron emission tomography/computed tomography scan for response evaluation. (a) Baseline maximum intensity projection 18F-fluorodeoxyglucose-positron emission tomography image shows metabolically active bilateral supraclavicular, bilateral axillary, mediastinal, and abdominopelvic lymphadenopathy suggestive of active tubercular pathology (baseline). (b) Baseline axial fluorodeoxyglucose-positron emission tomography/computed tomography images show enlarged right peribronchial, subcarinal, and left axillary lymphadenopathy with increased tracer uptake (baseline). (c) Axial fluorodeoxyglucose-positron emission tomography/computed tomography and (d) maximum intensity projection images show metabolic resolution of lymphadenopathy suggestive of complete metabolic response to anti-tubercular therapy

within the terminal ileum, along with narrowing and proximal dilatation. Other areas of small and large bowel involvement manifest as circumferential wall thickening, narrowing of the lumen, and ulceration. In the colon, involvement around the hepatic flexure is common. Physiological FDG uptake in the gut must be taken into account during any interpretation[8]

- Adrenal gland involvement: Asymmetrical enlargement with foci of increased FDG uptake. Later on, atrophy of the gland with calcifications can be seen [Figure 1][9]

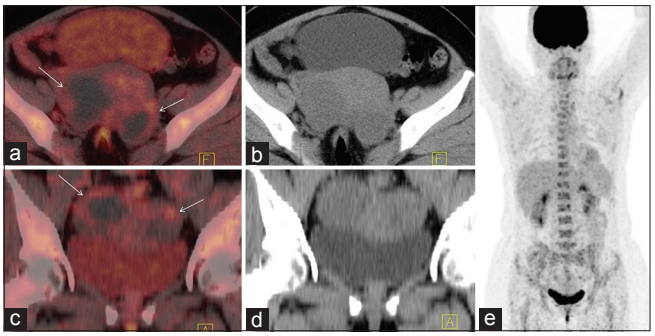

Figure 11: A 36-year-old female presented with genital tuberculosis. She received antitubercular therapy. She was referred for 18F-fluorodeoxyglucose-positron emission tomography/computed tomography scan. (a and b) Axial fluorodeoxyglucose-positron emission tomography/computed tomography and computed tomography, (c and d) Coronal fluorodeoxyglucose-positron emission tomography/computed tomography and computed tomography images show lobulated cystic masses in bilateral adnexae with increased tracer uptake in peripheral rim. (e) Maximum intensity projection 18F-fluorodeoxyglucose-positron emission tomography image shows metabolically active residual disease involving both tubo-ovarian masses

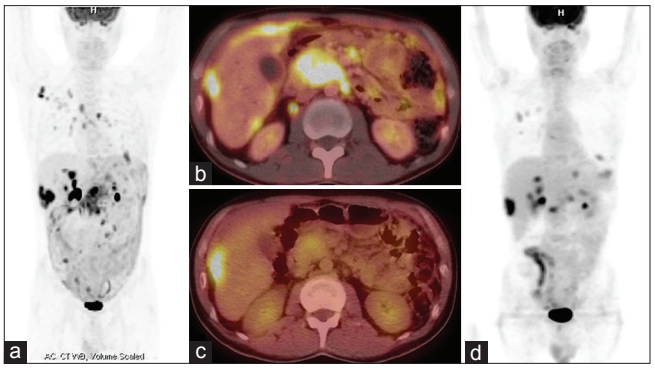

Figure 13: A 38-year-old male presented with disseminated tuberculosis. He was on antitubercular therapy. He was referred for 18F-fluorodeoxyglucose-positron emission tomography/computed tomography scan for response evaluation. (a) Baseline maximum intensity projection 18F-fluorodeoxyglucose-positron emission tomography image shows metabolically active liver lesions and abdominal and retroperitoneal lymphadenopathy suggestive of active tubercular pathology (baseline). (b) Baseline Axial fluorodeoxyglucose-positron emission tomography/computed tomography images show subcapsular liver lesions and peripancreatic and retroperitoneal lymphadenopathy with increased tracer uptake (baseline). (c) Axial fluorodeoxyglucose-positron emission tomography/computed tomography and (d) maximum intensity projection images show subcapsular liver lesions with increased radiotracer uptake suggestive of partial metabolic response to antitubercular therapy

- Hepatosplenic tuberculosis: Can occur as involvement in the form of FDG avid nodules or diffuse involvement which may be visualized as a "hot" liver/spleen [Figure 4][10]
- Urinary system tuberculosis: Usually in the form of Ulcerative and cavitary lesions showing FDG uptake. Complications such as papillary necrosis, scarring, and strictures may be seen. Postdiuretic imaging may aid visualization of lesions in the bladder and pelvicalyceal system[11,12]
- Genital tuberculosis: Testicular TB usually occurs due to direct extension from the urinary tract. Epididymal

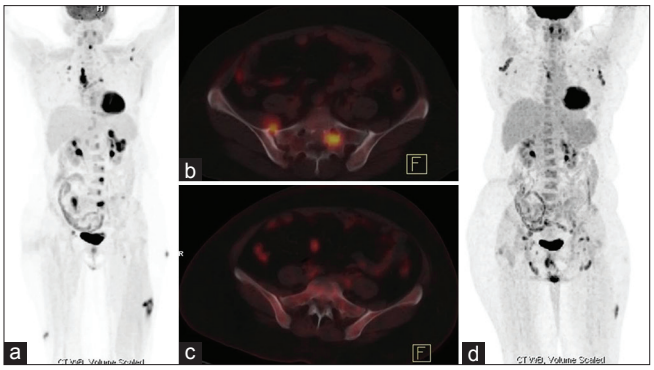

Figure 14: A 35-year-old female presented with extrapulmonary tuberculosis. She was on antitubercular therapy. She was referred for 18F-fluorodeoxyglucose-positron emission tomography/computed tomography scan for response evaluation. (a) Baseline maximum intensity projection 18F-fluorodeoxyglucose-positron emission tomography image shows metabolically active disease involving multiple skeletal sites suggestive of active tubercular pathology (baseline). (b) Baseline axial fluorodeoxyglucose-positron emission tomography/computed tomography images show lytic lesion in sacrum with increased tracer uptake (baseline). (c) Axial fluorodeoxyglucose-positron emission tomography/computed tomography and (d) maximum intensity projection images show metabolic resolution of disease to antitubercular therapy

extension may occur secondary to urinary TB or may occur hematogenously in children. Physiological FDG uptake in testis must be taken into consideration while evaluating involvement. Prostate can have TB through direct hematogenous extension.

Female genital TB most commonly occurs in the form of tubo-ovarian abscess which may be unilateral or bilateral [Figure 11]. Involvement of the uterus may also occur. Physiological uterine and ovarian uptake must be taken into account during evaluation of disease status.[12,13]

Assessment of Treatment Response

One of the principal areas of interest and relative strength of FDG-PET/CT lies in its potential utility for response evaluation in TB [Figures 12-14]. FDG-PET/CT imaging allows for both interim and end-of-treatment evaluations. Interim treatment response evaluations may facilitate estimation of the efficacy of treatment regimen and may potentially aid clinical decisions regarding treatment protocols and regimens. End-of-treatment evaluations are primarily aimed at searching for residual disease which may require further treatment.[14,15] This is more so true in the case of tubercular infections requiring long treatment durations (e.g., skeletal TB) in which drug toxicities are a greater concern.

Financial support and sponsorship

Nil.

Conflicts of interest

There are no conflicts of interest.

References

1. Cornelis F, Silk M, Schoder H, Takaki H, Durack JC, Erinjeri JP, *et al.* Performance of intra-procedural 18-fluorodeoxyglucose PET/CT-guided biopsies for lesions suspected of malignancy but poorly visualized with other modalities. Eur J Nucl Med Mol Imaging 2014;41:2265-72.
2. Fanchon LM, Dogan S, Moreira AL, Carlin SA, Schmidtlein CR, Yorke E, *et al.* Feasibility of *in situ*, high-resolution correlation of tracer uptake with histopathology by quantitative autoradiography of biopsy specimens obtained under 18F-FDG PET/CT guidance. J Nucl Med 2015;56:538-44.
3. Demura Y, Tsuchida T, Uesaka D, Umeda Y, Morikawa M, Ameshima S, *et al.* Usefulness of 18F-fluorodeoxyglucose positron emission tomography for diagnosing disease activity and monitoring therapeutic response in patients with pulmonary mycobacteriosis. Eur J Nucl Med Mol Imaging 2009;36:632-9.
4. Osborne MT, Hulten EA, Murthy VL, Skali H, Taqueti VR, Dorbala S, *et al.* Patient preparation for cardiac fluorine-18 fluorodeoxyglucose positron emission tomography imaging of inflammation. J Nucl Cardiol 2017;24:86-99.
5. Kilborn T, Janse van Rensburg P, Candy S. Pediatric and adult spinal tuberculosis: Imaging and pathophysiology. Neuroimaging Clin N Am 2015;25:209-31.
6. Sanei Taheri M, Karimi MA, Haghighatkhah H, Pourghorban R, Samadian M, Delavar Kasmaei H. Central nervous system tuberculosis: An imaging-focused review of a reemerging disease. Radiol Res Pract 2015;2015:202806.
7. Bhattacharya A, Kochhar R, Aggrawal K, Sharma S, Mittal BR. 18F-FDG and FDG-labeled leukocyte PET/CT in peritoneal tuberculosis. Clin Nucl Med 2014;39:904-5.
8. da Rocha EL, Pedrassa BC, Bormann RL, Kierszenbaum ML, Torres LR, D'Ippolito G. Abdominal tuberculosis: A radiological review with emphasis on computed tomography and magnetic resonance imaging findings. Radiol Bras 2015;48:181-91.
9. Roudaut N, Malecot JM, Dupont E, Boussion N, Visvikis D, Doucet L, *et al.* Adrenal tuberculosis revealed by FDG PET. Clin Nucl Med 2008;33:821-3.
10. Jeong YJ, Sohn MH, Lim ST, Kim DW, Jeong HJ, Chung MJ, *et al.* 'Hot liver' on 18F-FDG PET/CT imaging in a patient with hepatosplenic tuberculosis. Eur J Nucl Med Mol Imaging 2010;37:1618-9.
11. Merchant S, Bharati A, Merchant N. Tuberculosis of the genitourinary system-urinary tract tuberculosis: Renal tuberculosis-part II. Indian J Radiol Imaging 2013;23:64-77.
12. Engin G, Acunas B, Acunas G, Tunaci M. Imaging of extrapulmonary tuberculosis. Radiographics 2000;20:471-88.
13. Sharma JB, Karmakar D, Kumar R, Shamim SA, Kumar S, Singh N, *et al.* Comparison of PET/CT with other imaging modalities in women with genital tuberculosis. Int J Gynaecol Obstet 2012;118:123-8.
14. Martinez V, Castilla-Lievre MA, Guillet-Caruba C, Grenier G, Fior R, Desarnaud S, *et al.* (18)F-FDG PET/CT in tuberculosis: An early non-invasive marker of therapeutic response. Int J Tuberc Lung Dis 2012;16:1180-5.
15. Sathekge M, Maes A, Kgomo M, Stoltz A, Van de Wiele C. Use of 18F-FDG PET to predict response to first-line tuberculostatics in HIV-associated tuberculosis. J Nucl Med 2011;52:880-5.